enhancement. The change in fluorescence intensity of the LDL particle is observed with fluorescence microscopy and analyzed using single particle tracking. Dequenching events are observed as a single-step increase in intensity. Wortmannin, a drug that inhibits late endosome fusion, is used to block the transport of LDL to the lysosome. Individual dequenching events are not observed in wortmannin-treated cells suggesting that degradation of the LDL particle requires late endosome-lysosome interactions. This LDL labeling scheme will be extended to two-color single particle tracking experiments to determine the fraction of late endosome-lysosome interactions that lead to enzymatic degradation of LDL particles.

172-Pos Board B51

Activation Pathway Of paGFP In Living Cells

Ilaria Testa[1], Davide Mazza[1], Mario Faretta[2], Alberto Diaspro[1].
[1]IFOM MicroScoBio, Department of Physics-University of Genoa, Genoa, Italy, [2]IEO-IFOM Consortium for Oncogenomics, Milan, Italy.

Particle tracking inside the cell largely benefits of the ability to spatially and temporally mark specific structures to follow their ''signalling'' over a ''dark'' background as made possible since the advent of the photo-activatable markers. In terms of spatial confinement of the photo-activation process, the use of multiphoton excitation provides several favourable aspects compared to single photon confocal microscopy in photomarking biological structures to be tracked: the confined excitation volumes, of the order of magnitude of subfemtoliter, due to the non-linear requirements provide a unique control of the excitation and consequently photoactivation in the 3D space. In this context photoactivation experiments can be used to assess quantitative information about the binding kinetics of a macromolecule expressed in different cellular compartments. In this work we extended to photoactivation procedures and models originally developed for the quantitative analysis of FRAP experiments and we evaluated, for different proteins of medical interest (Rac-paGFP), the diffusive behaviour in the cytoplasm and the binding kinetics at the large endosomes. The results are compared with standard photobleaching experiments, in order to evidence the gained sensitivity obtained with photo-activatable proteins.

173-Pos Board B52

Organelle Specific Associations of HIV-1 Nef with HLA-I A2 and CD4 using Fluorescence Cross Correlation Spectroscopy

Tilman Rosales[1], Ling Yi[2], Jay R. Knutson[1], Sundararajan Venkatesan[2].
[1]National Institutes of Health, National Heart, Lung and Blood Institute, Bethesda, MD, USA, [2]National Institutes of Health, National Institute of Allergy and Infectious Diseases, Bethesda, MD, USA.

Among HIV encoded proteins, ***Nef*** is critically required for virus replication and AIDS pathogenesis and is a major effector of immune-evasion mechanisms, in part by modulating cell surface expression of CD4 and HLA-I receptors. Genetic and biochemical studies have suggested two different mechanisms for *Nef* induced downregulation of CD4 and HLA-I. This might reflect distinct and differential interactions between *Nef* and the receptors in the various subcellular organelles. To evaluate this possibility, we measured the interactions of *Nef* -cerulean with HLA-I A2-eYFP protein in the TGN, ER and plasma membrane in transiently transfected HeLa cells using single point Fluorescence Cross Correlation Spectroscopy (FCCS). We found that between 27 to 37% of the total concentration of *Nef* was found to be associated with HLA-I A2 in these organelles.

We also studied the interactions of a CD4-eYFP on the plasma membrane with *Nef*-cerulean. We found that most of the *Nef* present in the plasma membrane binds CD4. Two diffusion components for CD4 were observed, with most of the binding between CD4 and *Nef* occurring in the more mobile fraction. Most of the *Nef* at the plasma membrane was also found to bind CD4 LL/AA mutant, which is not downregulated by *Nef* efficiently and thus was thought to bind *Nef* less avidly. We also demonstrate that removal of cholesterol by β-methyl cyclodextrin abolished the larger complexes.

174-Pos Board B53

Raster Image Correlation Spectroscopy (RICS) with One Photon Excitation and Analog Detection: Some Practical Considerations for GUVs and Cell Membranes

M. vandeVen[1], E. Gielen[2], B. De Clercq[1], N. Smisdom[1], M. Ameloot[1].
[1]Hasselt University, Diepenbeek, Belgium, [2]Katholieke Universiteit Leueven and Hasselt University, Leueven and Diepenbeek, Belgium.

Raster Image Correlation Spectroscopy (RICS) allows for mapping the local translational diffusion coefficient(s). The applicability of the technique has recently been extended by implementation on confocal laser scanning microscopes (CLSM) having one-photon laser excitation and analog detection [1-4]. To better understand the reproducibility and accuracy of RICS analysis of cellular membranes and the top membranes of Giant Unilamellar Vesicles (GUVs) [4], the influence and the constraints imposed by instrumentation characteristics and by sample properties on the retrieved diffusion values have been simulated. Similarly to Brown et al [1], particle numbers in the observation volume and analysis brick size were varied. In addition the workable scan speed range was explored as well as the amount of allowed detection noise. We present evidence for a drop in D values when mapping towards the GUV perimeter and corroborate results when both the total number of particles and the mapping brick size get small. Experimental results show that the magnitude of correlated detection noise in our Zeiss LSM 510 META confocal system (build 2002) along the fast x-scan axis ($\psi = 0$) is considerably larger than reported by others [1-3]. The effect of omitting the $\psi = 0$ line in the analysis was investigated. Both the LFD, UCI RICS package as well as our Matlab software based on routines supplied by D. Kolin (McGill University) gave similar simulation and translational diffusion mapping results.

[1] Brown 2008, J. Microsc. *229*, 78-91.
[2] Dalal 2008, Microscopy Research and Technique *71*, 69-81.
[3] Sanabria 2008, Biophys J doi:10.1529/biophysj.108.138974.
[4] Gielen 2008, J. Fluoresc. *18*, 813-819.

175-Pos Board B54

Effects of Oversampling and Scanning Artifacts on the Accuracy of Spatial Fluorescence Intensity Fluctuation Analysis Methods

Mikhail Sergeev[1], Antoine G. Godin[1], Jody L. Swift[1], Yves De Koninck[1,2], Paul W. Wiseman[1].
[1]McGill University, Montreal, QC, Canada, [2]Centre de recherche Université Laval Robert-Giffard, Quebec, QC, Canada.

We present a systematic simulation and experimental study of potential measurement artifacts that arise due to raster scan acquisition for the image fluctuation analysis methods image correlation spectroscopy (ICS) and spatial intensity distribution analysis (SpIDA). With computer simulations, we show that photobleaching occurring during the sampling of sequential pixels affects the density and quantal brightness measurements obtained from single laser scanning microscopy images. This effect is even more pronounced when the images are oversampled with by using a small pixel size. The magnitude of this artifact was a function of the bleaching coefficients. The simulation results were compared to actual experimental data collected using a confocal laser-scanning microscope for a variety of dyes and sampling conditions. We analyzed images of monomeric fluorescent dyes covalently bound to coverslips, and monomeric green fluorescent protein (EGFP) transfected in mammalian cells. Moreover, we investigated the effects of non-constant emission of fluorescent probes, the presence of background noise and shot noise on the accuracy of the image fluctuation methods. We found that as the laser power increases (below saturation), some asymmetry in the spatial autocorrelation function appears which leads to systematic errors in the ICS measured number densities. SpIDA is also affected in the same manner by this artifact. Finally we looked at the accuracy of both techniques as a function of the quantal brightness of the particles. We generated computer simulated images of point emitters with different quantal brightness and then added shot noise to the images to determine accuracy and precision ranges for the measurements.

176-Pos Board B55

Biocompatible Quantum Dots for Intravital Kidney Imaging

Pu Wang[1], Daniel E. Minner[2], Keith M. Stantz[3], Christoph Naumann[2], **Weiming Yu**[4].
[1]Department of Physics, Indiana University-Purdue University Indianapolis, Indianapolis, IN, USA, [2]Department of Chemistry and Chemical Biology, Indiana University-Purdue University Indianapolis, Indianapolis, IN, USA, [3]Department of Radiology, Indiana University School of Medicine, Indianapolis, IN, USA, [4]Department of Physiology, Northwestern University, Feinberg School of Medicine, Chicago, IL, USA.

Quantum dots (QDs) are emerging alternatives to traditional dyes for fluorescence imaging applications. Quantum dots are attractive due to their photostability, broad excitation, narrow emission bands, high quantum yields and relatively long fluorescence lifetimes for contrast enhancement. We are interested in applying quantum dots (CdSe/ZnS) with biocompatible coatings for functional imaging of the kidney in vivo. Towards that end, we carried out experiments to characterize the bio- and photo-physical properties of CdSe/ZnS quantum dots with lipopolymer and aminoethoxy ethanol (AEE) coatings, and in vivo imaging of the kidney using surface coated quantum dots. We found that the fluorescence of the CdSe/ZnS quantum dots with surface coatings is enhanced in the presence of blood serum and it is serum concentration dependent. In addition, these surface coated quantum dots exhibit photo-induced fluorescence enhancement (PFE) and the PFE varies with specific surface coatings. Previously, PFE phenomenon is observed in CdSe quantum dots without surface coatings and has been studied under a number of different experimental conditions. To our knowledge, PFE of quantum dots with a surface coating has not been reported in the literature. For imaging application, we have

developed protocols to use these surface coated quantum dots for intravital imaging in rodents and we are able to successfully acquire in vivo images of the kidney and perform kinetic measurements. Here, we summarize and discuss our results of the PFE property and in vivo imaging and characterization of these quantum dots. This work was supported by NIH DK077051 research award to W. Yu on in vivo kidney imaging.

177-Pos Board B56

Time-lapse Imaging of Individual BK_{Ca} Channels in Live Cells Using Site-specific Labeling of Quantum Dots

Ji-Yeon Kim, **Haedeun Kim**, Sungho Chang, Chul-Seung Park.
GIST, Gwangju, Republic of Korea.

Although the proper localization of specific ion channels at certain regions of cell membrane is essential for their cellular functions, it is a great challenge to visualize and to trace individual channel proteins in live cells. We utilized quantum dots (QDs) to label the large-conductance Ca^{2+}-activated K^+ channels (BK_{Ca} channels) and monitored their movement in real-time. A site-specific biotinylation was achieved by genetically inserting the 'acceptor peptide' sequence at the extracellular N-terminus of the channel and by co-expressing the channel with the *E. coli* biotin-ligase modified to target into endoplasmic reticulum. After brief incubation of streptavidin-conjugated QDs, strong cell surface labeling of QDs was detected in both COS7 cell and cultured hippocampal pyramidal neurons. By tracking the labeled QDs using time-lapse imaging, we were able to monitor single BK_{Ca} channels with high resolution in live cells. In addition, two-color pulse-chase labeling allowed us to observe the channel trafficking to cell surface membrane *de novo* and their redistribution in real-time. Using the time-lapse imaging of QD-labeled channel protein as an assay system, we were able to show the differential roles of cytoskeletons in trafficking and dynamics of BK_{Ca} channels. This new approach can be applied to study the cellular behaviors of ion channels in many different aspects.

178-Pos Board B57

Non-Invasive Pyrenebutyrate-mediated Delivery of Quantum Dots to the Cytosol of Living Cells

Amy E. Jablonski, Christine K. Payne.
Georgia Institute of Technology, Atlanta, GA, USA.

Quantum dots are nanometer-diameter fluorescent probes made of semiconductor materials. Compared to organic fluorophores, quantum dots are highly photostable and very bright making them optimal for live cell imaging. A cationic peptide can be attached to the quantum dot giving an overall positive charge for cell surface binding and subsequent endocytosis. Once endocytosed into the cell, the quantum dots are trapped in vesicles and are unable to access cytosolic components. Pyrenebutyrate, an aromatic, hydrophobic molecule, interacts with the cationic peptide on the quantum dot creating a pyrenebutyrate-quantum dot complex that can bypass the endocytic pathway. The transport of the quantum dot across the plasma membrane is not inhibited at 4°C, lacks colocalization with endocytic markers, and has very little active motion within the cell. This suggests that the mechanism of transport is not endocytosis, but instead direct transport across the plasma membrane. A cell viability assay done with trypan blue determined that incubation with the highest concentration of pyrenebutyrate did not show any harmful effects. By bypassing the endocytic pathway this allows for targeting of cytosolic proteins difficult to label in live cells.

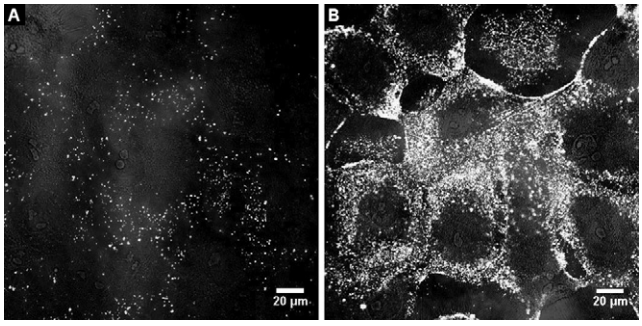

179-Pos Board B58

Characterizing the Architecture of Nicotinic Receptors with Quantum Dot-Based Fluorescence Microscopy

Rigo Pantoja[1], Erik A. Rodriguez[2], Shelly Tzlil[2], Larry Wade[1], Dennis A. Dougherty[2], Henry A. Lester[1].
[1]Division of Biology, Caltech, Pasadena, CA, USA, [2]Division of Chemistry and Chemical Engineering, Caltech, Pasadena, CA, USA.

Ion channel localization and trafficking is important for regulating excitability and synaptic transmission. Quantum dots (Qdots) coated with streptavidin were previously used to label membrane proteins that are recognized by biotinylated antibodies or by biotinylation of an acceptor peptide sequence. We report strategies, suitable for living cells, using strepatavidin-coated Qdots to count and locate extracellular domains of muscle and neuronal nicotinic acetylcholine receptors (nAChRs). Receptors were expressed in *Xenopus* oocytes. (1) The nonsense suppression methodology was used to incorporate the unnatural amino acid biocytin in the muscle nAChR α subunit, in the main immunogenic region, in place of the Asp70 residue. To accomplish this, the *T. thermophila* Gln amber suppressor (TQAS) was chemically aminoacylated with biocytin and co-injected with α70UAG:β:δ:γ mRNA. Functional expression was measured 24 - 48 hours post-injection. The muscle nAChR stoichiometry is $(\alpha)_2(\beta)_1(\delta)_1(\gamma/\varepsilon)_1$; in agreement, two colocalized Qdots were measured by blinking analysis with previously reported algorithms (Pantoja et al, Biophys J in press). (2) The muscle nicotinic receptor was labeled with α-bungarotoxin monoconjugated to biotin (α-Btx-Bio) and subsequently exposed to Qdots; some receptors exhibited the expected two Qdots. (3) The homopentameric α7 nAChR was labeled with α-Btx-Bio and subsequently labeled with Qdots. One to 3 Qdots per α7 receptor were detected, as expected from previous data. In all cases, the robust Qdot fluorescence enabled subunit localization with nanometer accuracy. Strategies (2) and (3) confirm that strategy (1), site-specific unnatural amino acid incorporation combined with Qdot labeling, provides a one-step, specific, efficient labeling approach to investigate composition and real-time trafficking of nicotinic receptors. Grants: NS11756, NS34407, HL79350. Fellowships: Ford and APA-DPN (RP), NSF (EAR).

180-Pos Board B59

HIV-virions Appear To Be Trapped By Human Cervical Mucus

Hacene Boukari, Beda Brichacek, Leonid Margolis, Ralph Nossal.
NIH, Bethesda, MD, USA.

We apply time-resolved fluorescence confocal microscopy and fluorescence correlation spectroscopy to examine the movements of fluorescently-labeled HIV-1 virions (~120 nm) embedded in crude human cervical mucus. Particle-tracking analysis indicates that the motion of most virions is decreased 200-fold compared to that in water and is not driven by typical diffusion. Rather, the time-dependence of their ensemble-averaged mean-square displacements is proportional to $\tau^{\alpha} + v^2\tau^2$, describing a combination of anomalous diffusion at short time scales ($\alpha \sim 0.3$) and flow-like behavior at longer times, τ being the lag time. We attribute the flow-like behavior to slowly-relaxing mucus matrix that follows mechanical perturbations such as stretching and twisting of the sample. Further analysis of the tracks and displacements of individual virions indicates differences in the local movements among the virions, including constrained motion and infrequent jumps, perhaps due to abrupt changes in matrix structure. We surmise that these differences are related not only to possible variations in the local microenvironments experienced by each individual virion but, perhaps, also to variations in the surface structure of the virions themselves. Possible changes in the microenvironments due to slow structural changes may provide a means for some virions to move and reach the port of entry, the underlying cervical mucosa.

Molecular Mechanics & Force Spectroscopy

181-Pos Board B60

Nucleosome Stacking Defines The Structural And Mechanical Properites Of Chromatin Fibers

Fan-Tso Chien[1], Maarten Kruithof[1], Andrew Routh[2], Daniela Rhodes[2], John van Noort[1].
[1]Leiden Institute of Physics, Leiden, Netherlands, [2]MRC Laboratory of Molecular Biology, Cambridge, United Kingdom.

In eukaryotic cells, genomic DNA, and core histones form dense 30 nm chromatin fibers. This compaction is driven by stacking of nucleosomes and has been implicated to regulate gene expression. We investigated the mechanical properties of reconstituted chromatin fibers containing 25 repeats of the 601 nucleosome-positioning element. The force-extension curves of these chromatin fibers were measured with magnetic tweezers. The fibers are well characterized by three springs in series: a worm like chain (WLC) of the flanking DNA, a Hookian spring of the 30 nm fiber, and a WLC of the ruptured fiber. Using this analysis we unambiguously demonstrated that nucleosome stacking drives a fiber with 197 bp repeat length into a solenoid helix. The model quantifies force dependent and Mg^{2+} dependent nucleosome unstacking, resolves the structural heterogeneity of 30 nm fiber folding, and reveals fivefold higher nucleosome-nucleosome interaction energy than reported before (Cui and Bustamante, 2000). This provides a complete structural and mechanical description of the high order folding of chromatin fibers.